

Supporting Information

Active Bromoaniline–Aldehyde Conjugate Systems and Their Complexes as Versatile Sensors of Multiple Cations with Logic Formulation and Efficient DNA/HSA Binding Efficacy: Combined Experimental and Theoretical Approach

Manik Das,^a Somali Mukherjee,^{b,*} Paula Brandao,^c Saikat Kumar seth,^d Santanab Giri,^e Soumya Sundar Mati,^f Bidhan Chandra Samanta,^g Soumik Laha,^h Tithi Maity^{a,*}

^a Department of Chemistry, P. K. College, Contai, Purba Medinipur, West Bengal 721404, India.

^b Department of Chemistry, University of Calcutta, 92, A. P. C. Road, Kolkata 700009, India.

^c Departamento de Química/CICEC, Universidade de Aveiro

^d Department of Physics, Jadavpur University, Kolkata, India.

^e Department of Chemistry, HIT, Haldia, India

^f Department of Chemistry, Government General Degree College, Keshiary, India

^g Department of Chemistry, Mugberia Gangadhar Mahavidyalaya, Purba Medinipur, West Bengal India

^h IICB, Kolkata

E-mail: titlipkc2008@gmail.com & somalimukherjee1993@gmail.com

Sl. No.	Index	Page No.
1.	IR spectrum of complex 1 and 2 (Figure S1)	S3
2.	UV spectrum of complex 1 and 2 (Figure S2)	S3
3.	Selected bond lengths and angles table of complex 1 and 2 (Table S1)	S4
4.	Change of fluorescence intensity after addition of different analysts (60 μM) to a fixed concentration of ligand HL ₁ and HL ₂ (40 μM) DMSO/H ₂ O HEPES buffer solution (Figure S3)	S4
5.	Stern-Volmer graph for detection of quenching constant of HL ₁ after addition of Cu ²⁺ ion (Figure S4)	S5

6.	Change of Fluorescence emission intensity of (a) HL₁ as a function of Cu ²⁺ ion and (b) HL₂ as a function of Zn ²⁺ ion for detection limit calculation (Figure S5)	S5
7.	UV spectral titration of (a) HL₁ with Cu ²⁺ and (b) HL₂ with Zn ²⁺ ion solution respectively (Figure S6)	S6
8.	Stability in DMSO/H ₂ O 9:1 HEPES buffer medium at different pH and the stability in DMSO/water (9:1) solvent at a fixed pH value (7.4) by means of time–scan experiment of (a) HL₁ and (b) HL₂ (Figure S7)	S6
9.	Naked eye colour changes after addition of Al ³⁺ and Hg ²⁺ to complex 2 in the presence of different cations in 9:1 (DMSO/H ₂ O) HEPES buffer (pH = 7.4) solution (Figure S8)	S7
10.	Stern-Volmer graph for detection of quenching constant of complex 2 after addition of (a) Al ³⁺ ion and (b) Hg ²⁺ ion (Figure S9)	S7
11.	Change of Fluorescence emission intensity of complex 2 as a function of (a) Al ³⁺ ion and (b) Hg ²⁺ ion for detection limit calculation (Figure S10)	S8
12.	Absorption titration spectra of (a) complex 1 (b) complex 2 in absence and presence of ct-DNA. Inset: best fitting graph for binding affinity calculation (Figure 11)	S8
13.	Change of Emission spectra of the ctDNA-EtBr complex with addition of increasing concentration of (a) Complex 1 (b) Complex 2 and in inset the fractional fluorescence (F ⁰ /F) plot of CT-DNA-EtBr as a function concentration of the complexes (Figure S12)	S9
14.	Change of Emission spectra of the ctDNA-DAPI complex with addition of increasing concentration of (a) Complex 1 (b) Complex 2 and in inset the fractional fluorescence (F ⁰ /F) plot of CT-DNA-DAPI as a function concentration of the complexes (Figure S13)	S9
15.	CD spectra of ctDNA in CP buffer in the presence and absence of (a) complex 1 and (b) 2 (Figure 14)	S10
16.	UV-Vis spectral analysis of complexes in tris buffer medium (Figure S15)	S10
17.	Docked binding energy and other parameters of complex 1 and complex 2 with HSA and ctDNA (Table S2)	S11

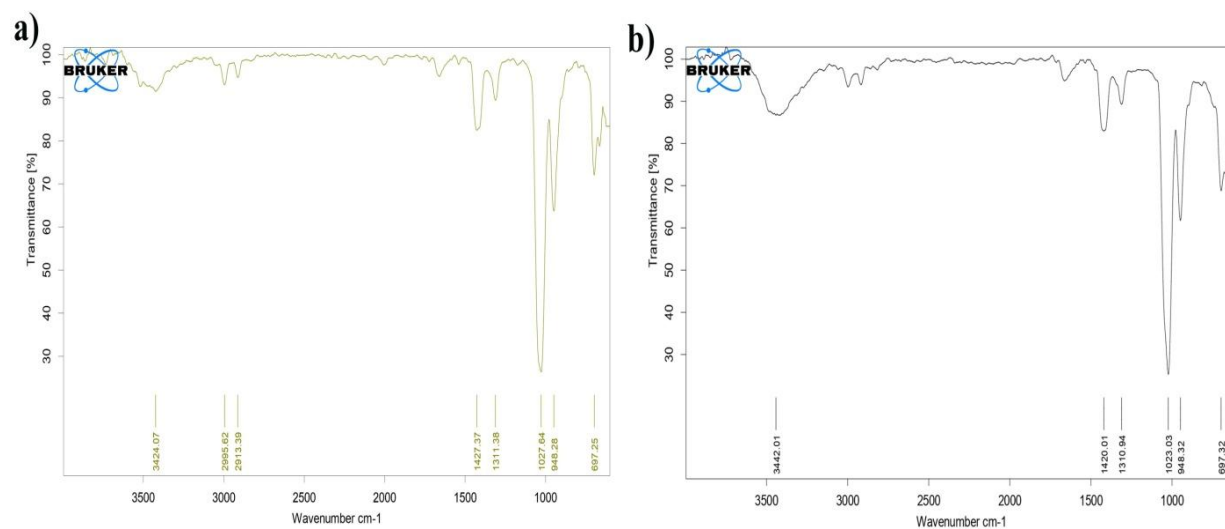


Figure S1. IR spectrum of complex (a) **1** and (b) **2**.

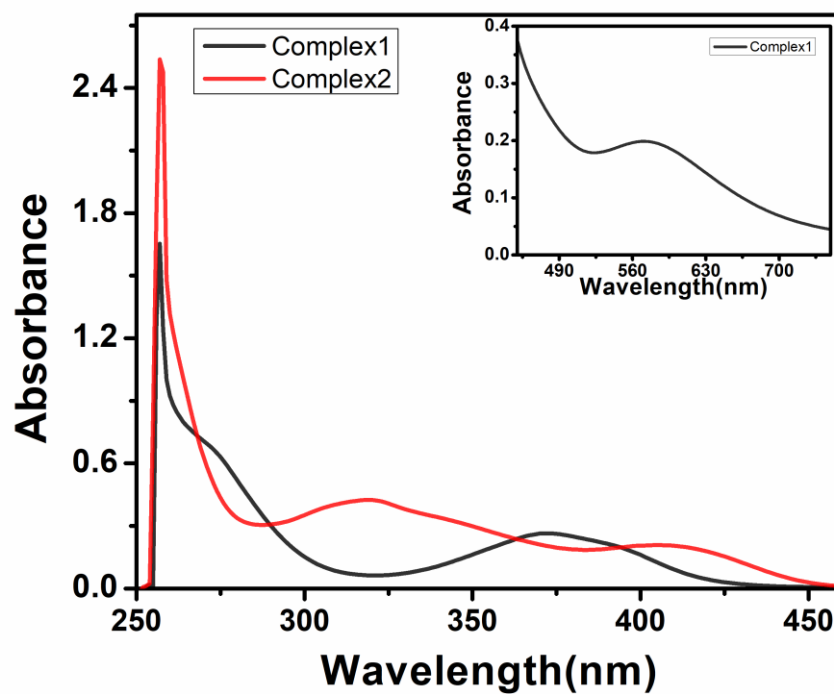


Figure S2. UV spectrum of complex **1** and **2**.

Table S1. Selected bond length and bond angle table of Complex **1** and **2**.

Bond length (Å)			
Complex 1		Complex 2	
Cu1-O1	1.888(4)	Zn1-O1	1.899(3)
Cu1-N1	2.011(3)	Zn1-N1	2.022(3)
Bond angle (°)			
Complex 1		Complex 2	
O1-Cu1-N1	90.83(14)	O1-Zn1-N1	96.60(11)
O1-Cu1-N1a	89.17(14)	N1-Zn1-N1a	122.03(11)
N1-Cu1-N1a	180	O1-Zn1-O1a	119.60(12)
O1-Cu1-O1a	180.	O1-Zn1-N1a	111.87(11)

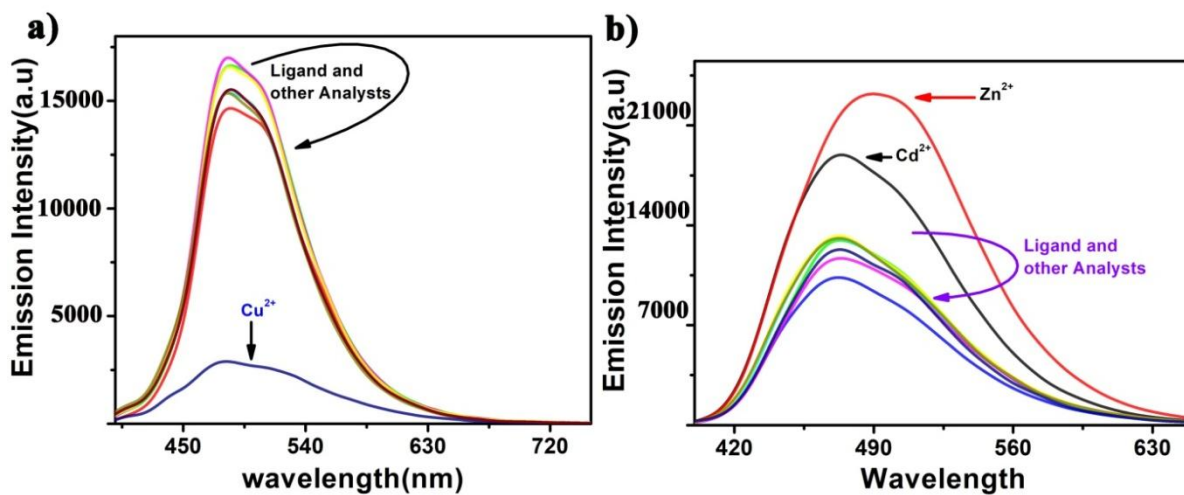


Figure S3. Change of fluorescence intensity after addition of different analytes (60 μM) to a fixed concentration of ligand (a) **HL₁** and (b) **HL₂** (40 μM) DMSO/H₂O

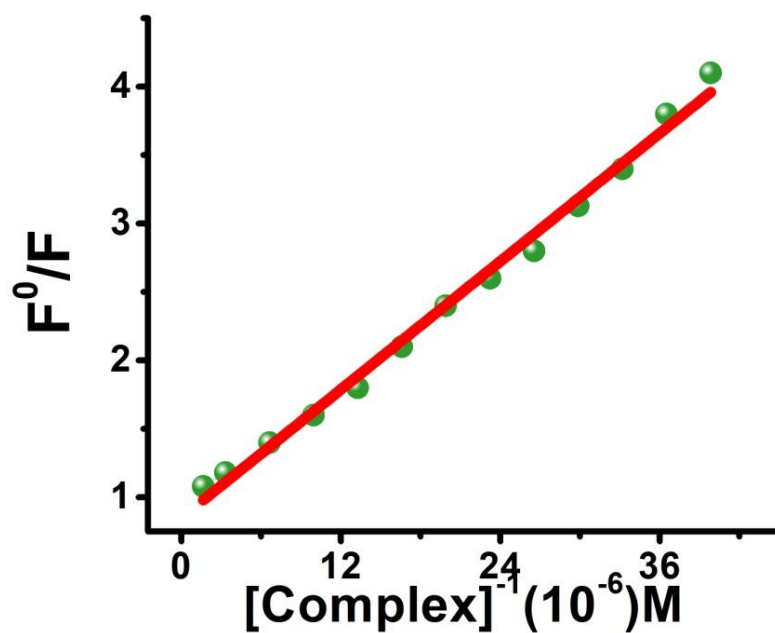


Figure S4. Stern-Volmer graph for determination of quenching constant of **HL₁** after addition of Cu^{2+} ion.

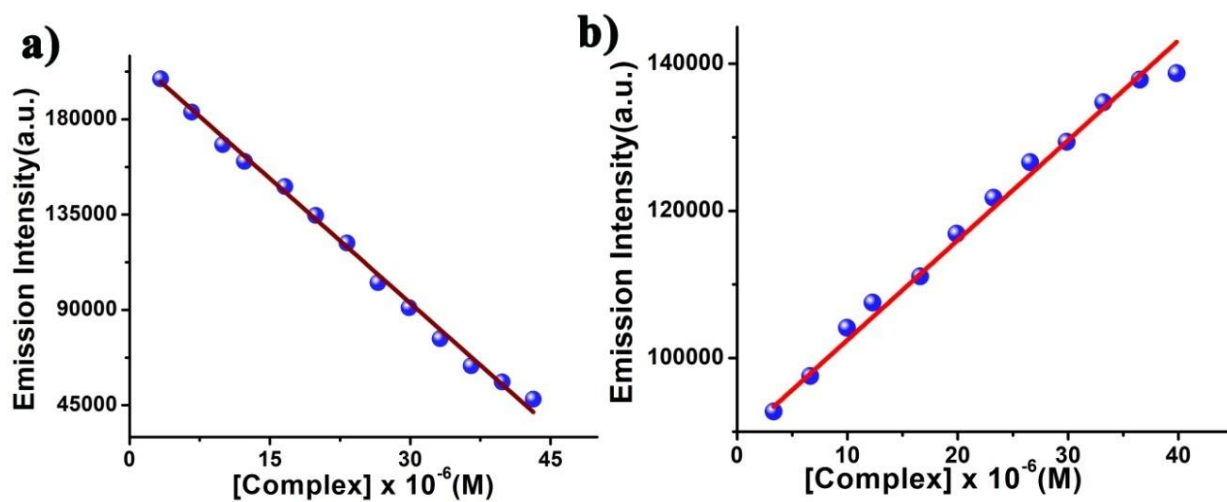


Figure S5. Change of Fluorescence emission intensity of (a) **HL₁** as a function of Cu^{2+} ion and (b) **HL₂** as a function of Zn^{2+} ion for detection limit calculation.

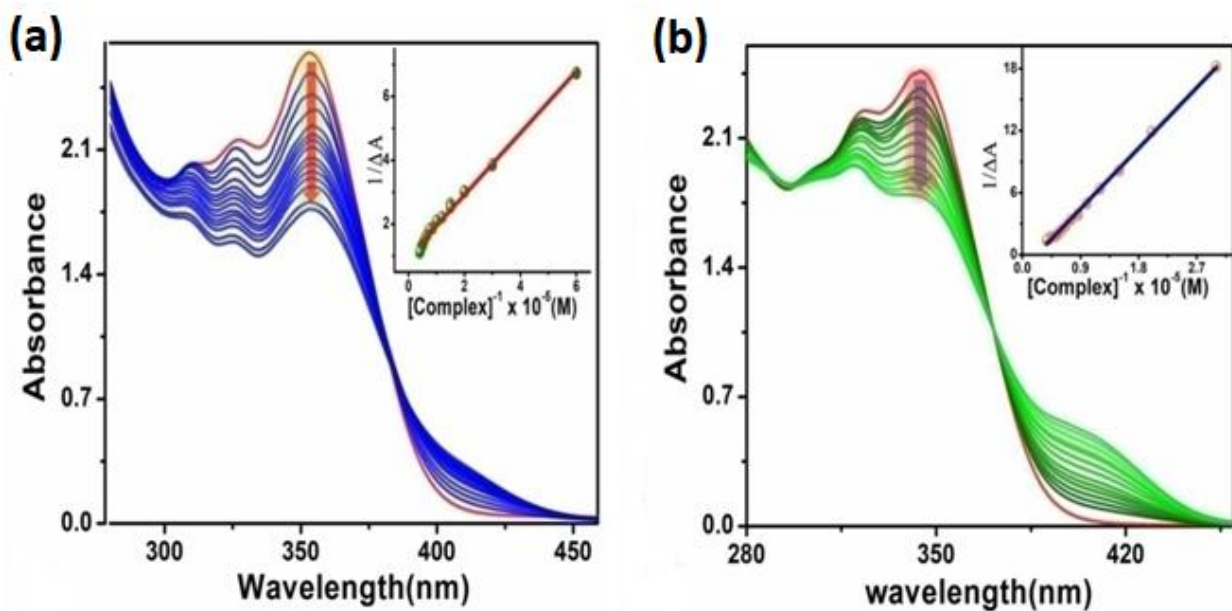


Figure S6. UV spectral titration of (a) **HL₁** with Cu²⁺ and (b) **HL₂** with Zn²⁺ ion solution respectively.

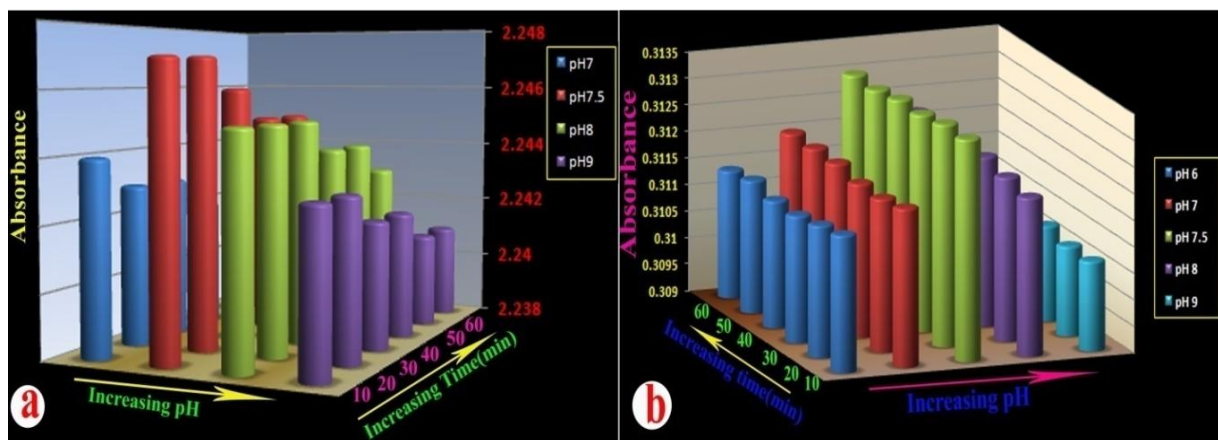


Figure S7. Stability in DMSO/H₂O (9:1) HEPES buffer medium at different pH and the stability in DMSO/water (9:1) solvent at a fixed pH value (7.4) by means of time-scan experiment of (a) **HL₁** and (b) **HL₂**

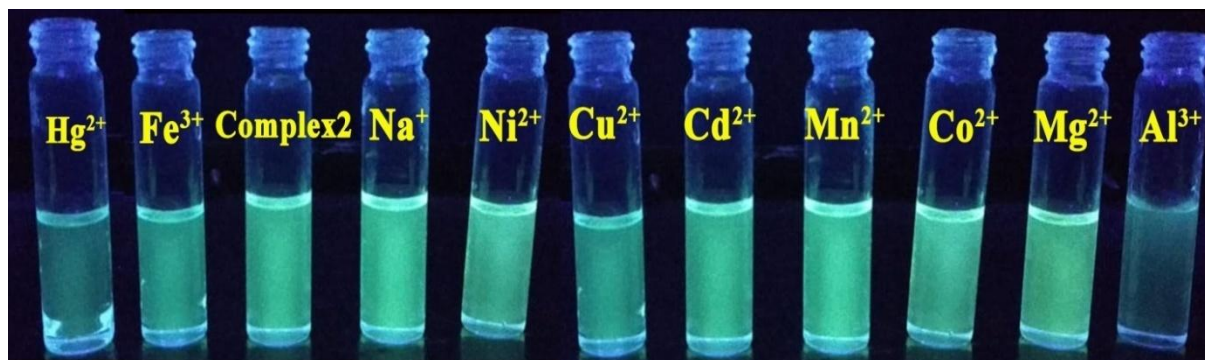


Figure S8 Naked eye colour changes after addition of Al^{3+} and Hg^{2+} to complex **2** in the presence of different cations in 9:1 (DMSO/ H_2O) HEPES buffer (pH = 7.4) solution.

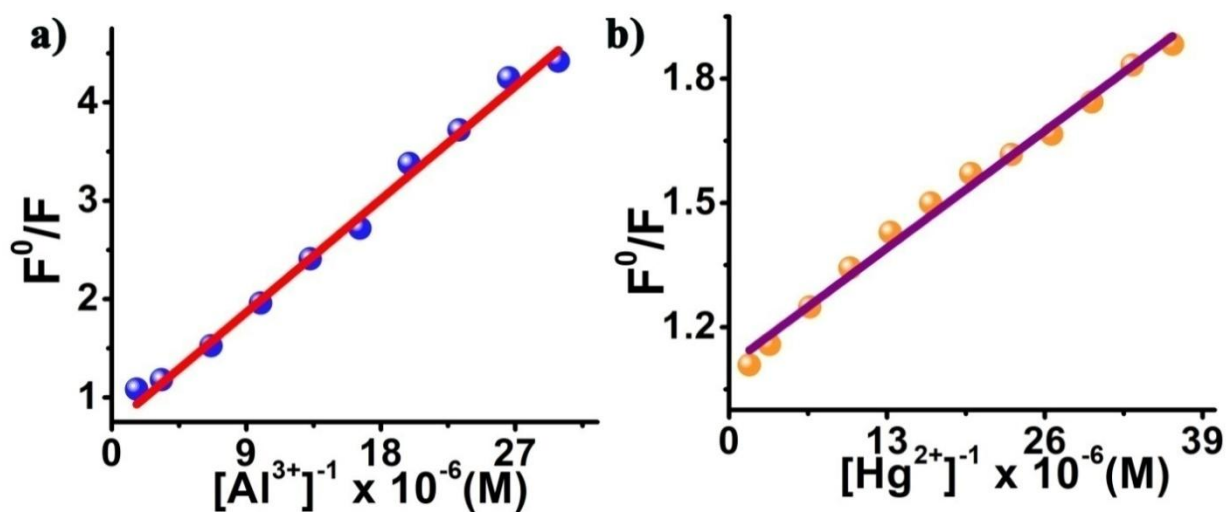


Figure S9. Stern-Volmer graph for detection of quenching constant of complex **2** after addition of (a) Al^{3+} ion and (b) Hg^{2+} ion.

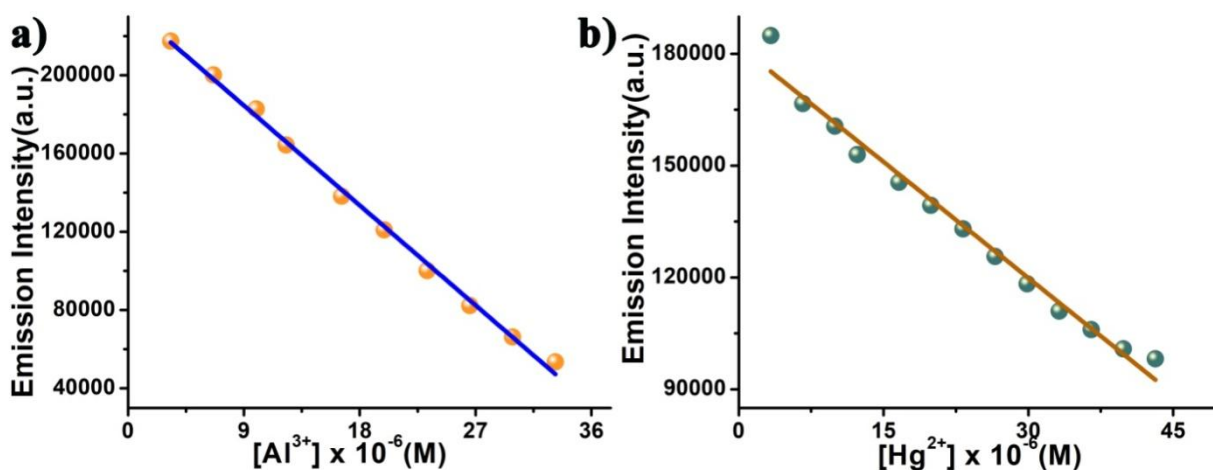


Figure S10. Change of fluorescence emission intensity of complex **2** as a function of (a) Al^{3+} ion and (b) Hg^{2+} ion for detection limit calculation.

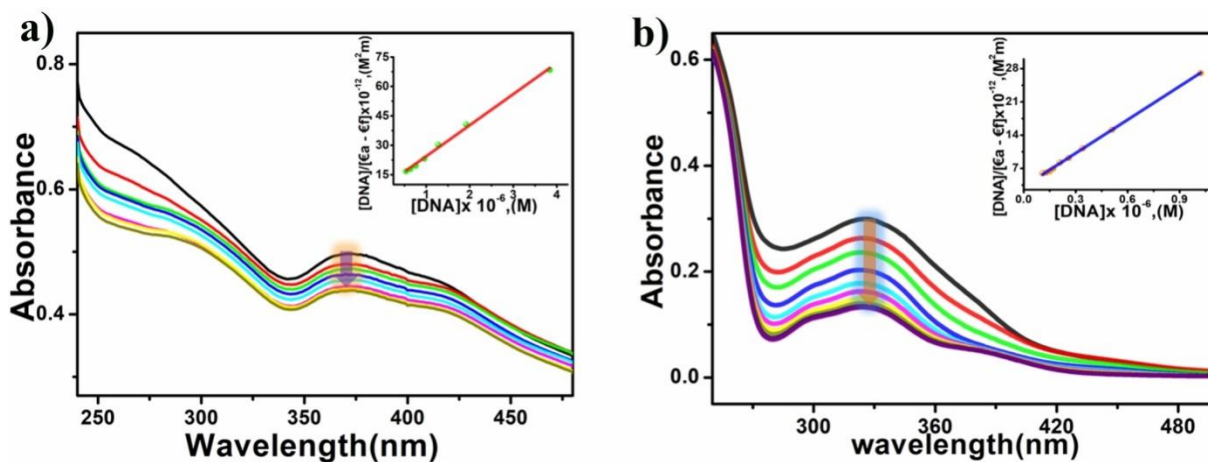


Figure 11. Absorption titration spectra of (a) complex **1** (b) complex **2** in absence and presence of ct-DNA. Inset: best fitting graph for binding affinity calculation.

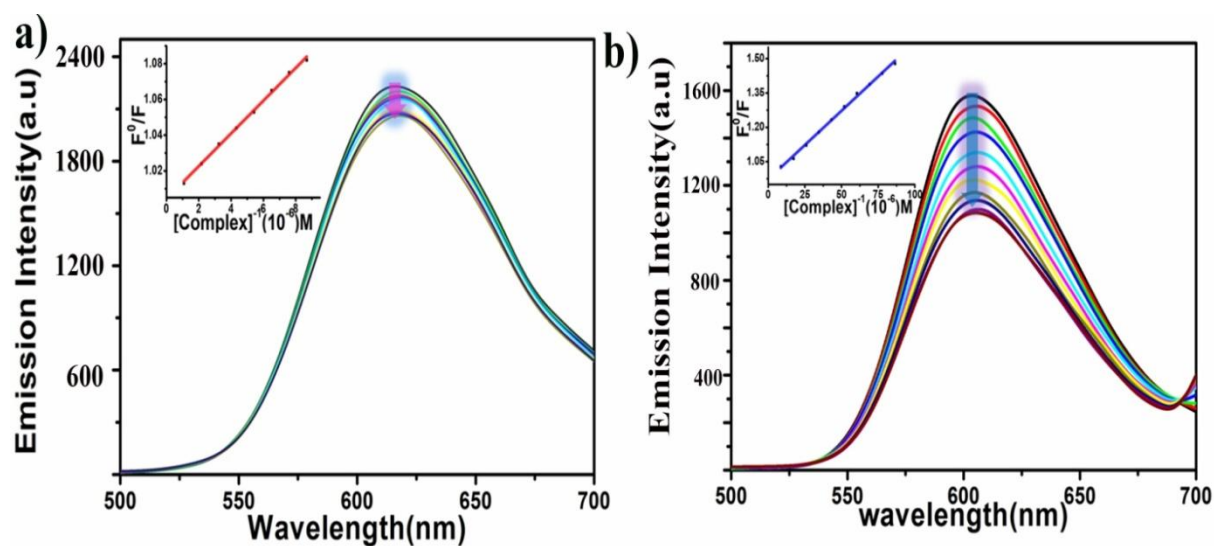


Figure S12. Change of Emission spectra of the ctDNA-EtBr complex with addition of increasing concentration of (a) Complex 1 (b) Complex 2 and in inset the fractional fluorescence (F^0/F) plot of CT-DNA-EtBr as a function concentration of the complexes.

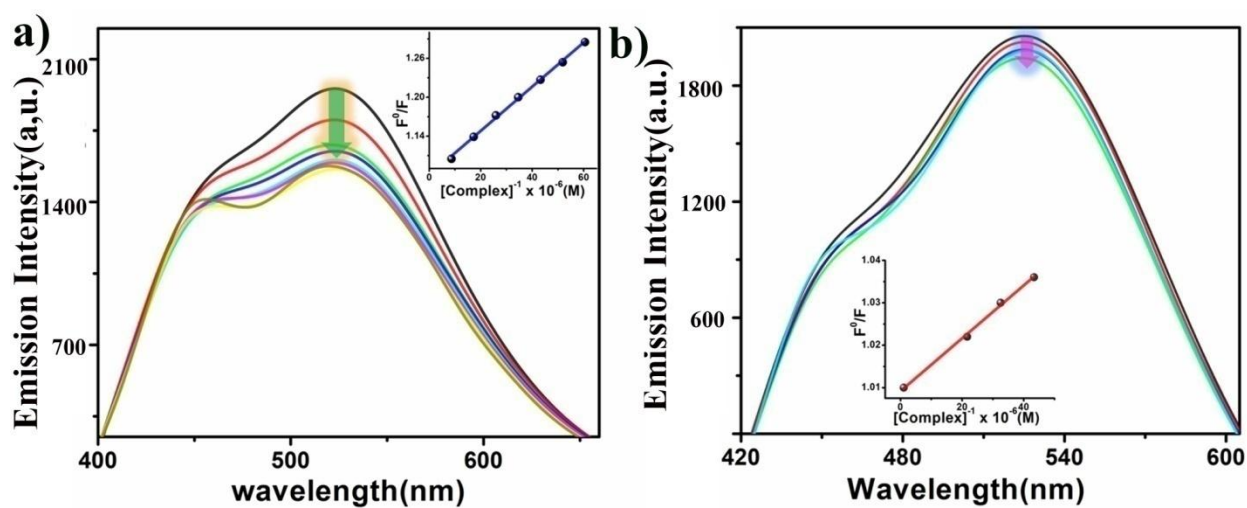


Figure S13. Change of Emission spectra of the ctDNA-DAPI complex with addition of increasing concentration of (a) Complex 1 (b) Complex 2 and in inset the fractional fluorescence (F^0/F) plot of CT-DNA-DAPI as a function concentration of the complexes.

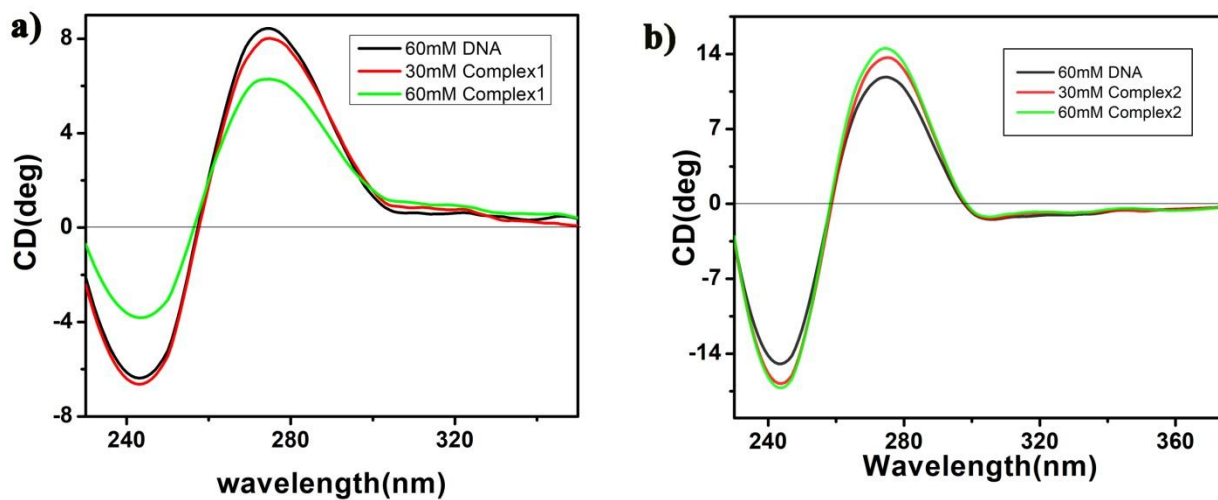


Figure S14. CD spectra of ctDNA in CP buffer in the presence and absence of (a) complex 1 and (b) 2

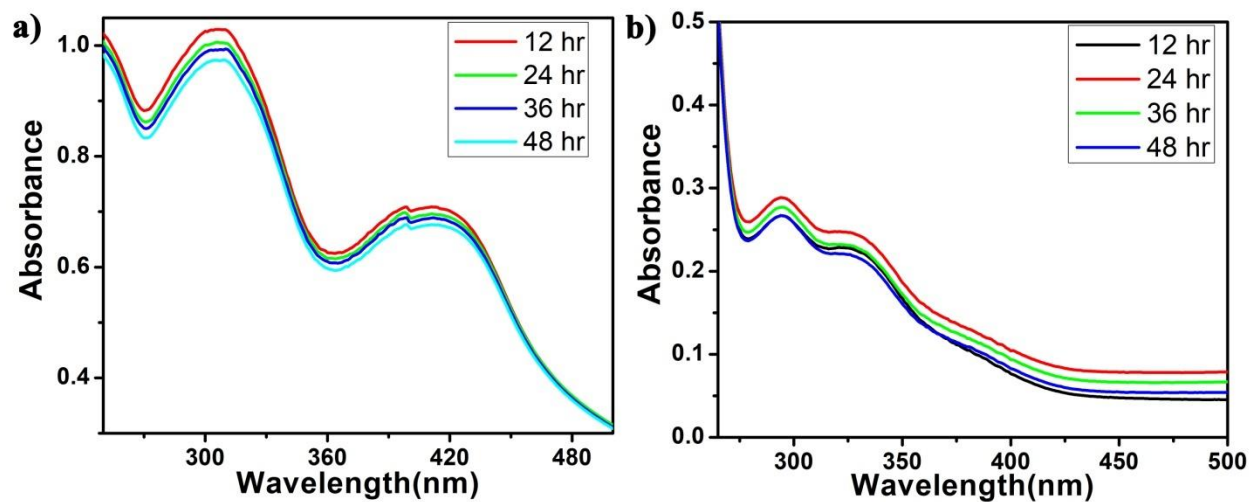


Figure S15. UV-Vis spectral analysis in tris buffer medium of (a) complex 1 and (b) 2.

Table S2. Docked binding energy and other parameters of complex **1** and complex **2** with HSA and ctDNA.

HSA			
Complex	Binding energy (kcal/mol)	Ligand Efficiency	Intermolecular Energy (kcal/mol)
1	-8.96	-0.26	-9.55
2	-8.29	-0.25	-8.89
ctDNA			
Complex	Binding energy (kcal/mol)	Ligand Efficiency	Intermolecular Energy (kcal/mol)
1	-5.61	-0.22	-6.20
2	-5.96	-0.26	-6.55
